Electrical Resistance of a Capillary Endothelium

CHRISTIAN CRONE and OVE CHRISTENSEN

From the Institute of Medical Physiology, University of Copenhagen, The Panum Insitute, DK-2200 Copenhagen N, Denmark

ABSTRACT The electrical resistance of consecutive segments of capillaries has been determined by a method in which the microvessels were treated as a leaky, infinite cable. A two-dimensional analytical model to describe the potential field in response to intracapillary current injection was formulated. The model allowed determination of the electrical resistance from four sets of data: the capillary radius, the capillary length constant, the length constant in the mesentery perpendicular to the capillary, and the relative potential drop across the capillary wall. Of particular importance were the mesothelial membranes covering the mesenteric capillaries with resistances several times higher than that of the capillary endothelium. 27 frog mesenteric capillaries were characterized. The average resistance of the endothelium was 1.85 Ωcm^2, which compares well with earlier determinations of the ionic permeability of such capillaries. However, heterogeneity with respect to resistance was observed, that of 10 arterial capillaries being 3.0 Ωcm^2 as compared with 0.95 Ωcm^2 for 17 mid- and venous capillaries. The average in situ length constant was 99 μm for the arterial capillaries and 57 μm for the mid- and venous capillaries. It is likely that the ions that carry the current must move paracellularly, through junctions that are leaky to small solutes.

INTRODUCTION

Most studies of the permeability of single capillaries have been undertaken with the Landis occlusion technique (Landis, 1927), or modifications of it (Michel et al., 1974). The technique allows determination of filtration coefficients and reflection coefficients to various solutes (Curry et al., 1976). Crone and Friedman (1976) introduced electrophysiological methods in studies of ionic permeability of single capillaries using ion-sensitive microelectrodes. From this experimental approach arose the idea of studying the electrical resistance of the capillary wall by injecting current into the capillary and monitoring the electrical potential field created inside and outside the capillary in response to the current (Crone, 1980). In the present paper, we report the theoretical analysis and experimental results obtained in a series of experiments in which the electrical resistance of microvessels in the frog mesentery was determined. The analysis rests on an analogy between a blood capillary

J. GEN. PHYSIOL. © The Rockefeller University Press · 0022-1295/81/04/0349/23 $1.00 349
Volume 77 April 1981 349-371

and a leaky, infinite electric cable—the capillary wall corresponding to the insulating mantle and the plasma to the inner core.

This approach to capillary permeability opens up the possibility of studying fast changes in capillary wall resistance and unspecific ionic permeability—a territory which so far has been unapproachable because of methodological limitations. In this paper, however, we restrict ourselves to an account of the determination of the electrical constants.

THEORY

In one-dimensional cable theory the decline of transmembrane potential in response to a steady current is logarithmic under certain simplified conditions (Eisenberg and Johnson, 1970). Thus, $V(x) = V(0) \exp(-x/\lambda)$, where $V(x)$ is the steady displacement of membrane potential at a distance x from the site of injection of current into an infinitely long cable. $V(0)$ is the potential at the point of current injection and λ is the length constant. Under conditions under which the fluid by which the leaky cable is surrounded has a high conductance, the length constant is given by $\sqrt{r_m/r_i}$, where r_i is the core resistance (Ωcm^{-1}) and r_m is the resistance per unit length of the semiinsulating sheath (Ωcm). To the extent that these simple requirements are fulfilled, a similar analysis can in principle be used for determination of the electrical resistance of the capillary wall. Current is injected into the capillary, and the resulting potential displacement is measured at various distances from the current source within the capillary.

In practice, the geometrical conditions in the frog's mesentery differ in several respects from those required in simple cable theory, the most significant difference being that the capillaries lie between two mesothelial membranes that cover the mesentery and that have electrical resistances comparable to that of the capillary wall (Frøkjær-Jensen and Christensen, 1979). Thus, a supplementary analysis is required to describe the current-voltage relations in a mesenteric capillary. Although special conditions exist in the mesentery, the essence of the method may be applied to other tissues in which the geometry is less complicated and closer to that of a leaky cable suspended in a conducting medium. Before giving an analysis of the special conditions in the mesentery, it is convenient to review some of the fundamental relations for a "naked" capillary surrounded by a medium of high conductance.

The capillary is characterized by two important parameters. The first is the resistance of a 1-cm^2 capillary wall to current flowing perpendicularly through the wall, R_m (Ωcm^2). The surface area per centimeter of capillary length is $2\pi a$ (cm^2/cm), where the capillary radius is a. Thus, the membrane resistance per centimeter of capillary length, r_m, is given by

$$r_m = \frac{R_m}{2\pi a} \ (\Omega cm).$$

When the inner medium in the capillary has a resistivity of ρ_i (Ωcm), the internal resistance per centimeter of capillary length, r_i, is given by

$$r_i = \frac{\rho_i}{\pi a^2} \ (\Omega cm^{-1})$$

for current flowing longitudinally within the capillary.

When current is injected into a tubular structure, the potential variation, $V(x)$, inside the capillary (x-direction) is governed by the field equation (Hodgkin and Rushton, 1946)

$$\frac{1}{r_i}\frac{d^2V}{dx^2} = \frac{1}{r_m} \cdot V(x). \tag{1}$$

Letting $\sqrt{r_m/r_i} = \lambda_x$, the field equation is $d^2V/dx^2 = (1/\lambda_x^2)V$, with the familiar solution

$$V(x) = V(0)e^{-x/\lambda_x} \tag{2}$$

for current injected at $x = 0$.

λ_x is the experimentally determined figure from which the capillary wall resistance can be calculated using the relation

$$R_m = r_i \cdot \lambda_x^2 \cdot 2\pi a \tag{3}$$

derived from the preceding equations.

Field Equation for a Mesenteric Capillary

Current injected into a mesenteric capillary returns to the superfusate covering the upper mesenteric surface along two paths (cf. Fig. 1). One is through the upper part of the capillary circumference and the mesothelium covering it. The other is sidewards via the lateral parts of the capillary wall into the interstitium between the mesothelial membranes and back through the upper mesothelial membrane to the superfusate.

In the following analysis the well-superfused upper surface of the mesentery is considered to be equipotential (zero). It is further assumed that no current leaks in the downward direction, because the fluid layer between the lower mesothelial membrane and the perspex pillar on which the mesentery is mounted is negligible (Frøkjær-Jensen and Christensen, 1979). The symbols used in the model are defined in the following list.

SYMBOL	UNIT	DESCRIPTION
R_m	Ωcm^2	Specific resistance of endothelial wall
r_m	Ωcm	Resistance per centimeter of capillary wall
ρ_i	Ωcm	Resistivity of capillary interior
R_{mes}	Ωcm^2	Specific resistance of mesothelial membrane
ρ_o	Ωcm	Resistivity of interstitium
r_i	Ωcm^{-1}	Resistance of 1 cm of capillary interior
r_{lat}	Ωcm	Resistance of 1 cm of capillary wall, facing interstitium
r_{up}	Ωcm	Resistance of 1 cm of upward-facing capillary wall and covering mesothelium

r_o	Ω	Resistance of a square slab of mesentery
λ	cm	Length constant of "naked" capillary
λ_x	cm	Length constant for potential variation in direction x, in both capillary and interstitium
λ_y	cm	Length constant for potential variation perpendicular to capillary in interstitium
λ_{mes}	cm	Length constant of mesothelial membrane
h	cm^{-1}	$=\rho_o/R_m$
a	cm	Capillary radius
d	cm	Thickness of mesentery
$V(x)$	V	Potential in capillary at position x
$V_{out}(x, y)$	V	Potential in interstitium, referred to tip of current-injecting electrode

To set up the differential equation describing the current flow within and out of the capillary, two resistances consistent with the model described above must be defined (cf. Fig. 1), r_{up} and r_{lat} (per centimeter of capillary length). In analogy with the equation for the "naked" capillary (Eq. 1), the field equation for the "wrapped" capillary is

$$\frac{1}{r_i}\frac{d^2V}{dx^2} = \frac{1}{r_{lat}}[V(x) - V_{out}(x, 0)] + \frac{1}{r_{up}}V(x), \tag{4}$$

where V_{out} $(x, 0)$ is the potential in the interstitium immediately outside the capillary ($y = 0$). The first term on the right-hand side is current leaking from capillary to interstitium and is equal to the potential difference across the capillary divided by the lateral capillary resistance. The second term is current leaking upward through both the capillary wall and mesothelium. The term on the left-hand side gives the negative rate of change with distance of current flowing in the capillary.

To evaluate r_{lat} and r_{up}, we assume that the mesothelium is tightly wrapped around a capillary, leaving a free capillary surface in the lateral directions. The "height" of the free surface equals that of the interstitium outside the capillary, d, which is always smaller than the diameter of the capillary (cf. Fig. 1). Current from capillary to interstititum passes (per centimeter) through the area $2d$; therefore,

$$r_{lat} = R_m/2d. \tag{5}$$

The current leaving upward passes through an area (per centimeter) approximately half the circumference minus d. Thus,

$$r_{up} = (R_m + R_{mes})/(\pi a - d), \tag{6}$$

where R_{mes} is the specific resistance of the mesothelial membrane.

Field Equation for the Interstitium

The resistance of a square slab of interstitium of thickness d is $r_o = \rho_o/d$, where ρ_o is the resistivity of the interstitium. The unit for r_o is ohm, often denoted

ohm per square ($\Omega/\square$). In the interstitium, current flows in two dimensions, so that the field equation is given by

$$\frac{1}{r_o}\left(\frac{\partial^2 V_{out}}{\partial x^2} + \frac{\partial^2 V_{out}}{\partial y^2}\right) = \frac{1}{R_{mes}} \cdot V_{out}(x, y), \tag{7}$$

where V_{out} (x, y) is the potential field in the mesentery. The y-coordinates lie perpendicular to the capillary. This equation is analogous to the field equation for the naked capillary (Eq. 1), except that it accounts for two-dimensional current flow. The ratio R_{mes}/r_o may be interpreted as the square of a length constant for the mesothelial membrane, λ_{mes}.

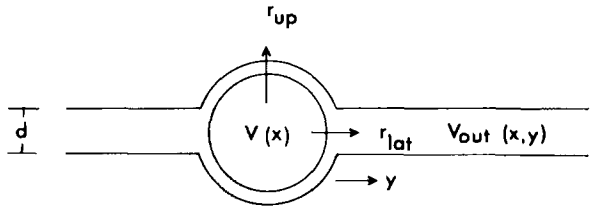

FIGURE 1. Schematic representation of a capillary lying between two mesenteric membranes. Current injected into the capillary creates a potential $V(x)$ that is attenuated as a result of current flow through two resistances, r_{up} and r_{lat}. r_{up} is due to two successive membranes, the capillary wall and the covering mesothelium. The current flowing into the interstitium in the lateral direction creates a potential field, V_{out} (x, y). d is the average height of the interstitium.

Boundary Condition

At any given position in the capillary the current leaving the vessel must equal the interstitial current component in the y-direction immediately outside the capillary, at $y = 0$. This boundary condition is expressed in the following equation:

$$i_y(x, 0) = \frac{V(x) - V_{out}(x, 0)}{R_m} = -\frac{1}{\rho_o} \cdot \left.\frac{\partial V_{out}}{\partial y}\right|_{y=0}, \tag{8}$$

which expresses the current density perpendicular to the capillary and connects the fields $V(x)$ and $V_{out}(x, y)$ described by Eqs. 4 and 7.

Eqs. 4, 7, and 8 represent a set of coupled differential equations that can be solved analytically to give the potential variations within the capillary and in the interstitium,

$$V(x) = V(0) \exp(-x/\lambda_x), \quad (x \geqq 0) \tag{9a}$$

and

$$V_{out}(x, y) = V(0) \frac{h\lambda_y}{1 + h\lambda_y} \exp\left[-\left(\frac{x}{\lambda_x} + \frac{y}{\lambda_y}\right)\right], \quad \left(\frac{x}{y} \geqq 0\right), \tag{9b}$$

where $h = \rho_o/R_m$ (cm^{-1}), and λ_x and λ_y are the length constants along the x-axis and y-axis. Within the capillary the potential variation in the y-direction is ignored. The potential is symmetric with respect to the coordinate axes. Notice that λ_x is the same within and outside the capillary. The potential at the outside of the capillary wall is a constant fraction of the potential within the capillary at any point, and the ratio between the two potentials is given by $h\lambda_y/(1 + h\lambda_y)$.

The field is completely characterized by the three quantities λ_x, λ_y, and h, all of which are determined experimentally. From these measured quantities, the sought resistance of the capillary endothelium, R_m, is obtained by use of Eq. 10, itself derived by insertion in the earlier equations (for details, see Appendix),

$$r_{lat} = r_i \cdot \lambda_x^2 \left[\frac{1}{1 + h\lambda_y} + \frac{\pi a - d}{2(d + h\lambda_{mes}^2)} \right], \tag{10}$$

where the length constant of the mesothelium is related to λ_x and λ_y by the equation $1/\lambda_x^2 + 1/\lambda_y^2 = 1/\lambda_{mes}^2$. Eq. 10 is the familiar cable equation, with a multiplication factor contained within the brackets.

Finally, the resistance of the capillary membrane, R_m, is obtained from the relationship (cf. eqs. 3 and 5)

$$R_m = 2d \cdot r_{lat}. \tag{11}$$

The procedure in data evaluation is thus to start with the measured values λ_x and λ_y together with the ratio of potentials inside and just outside the capillary. The two first quantities define λ_{mes}, and the potential ratio gives $h\lambda_y$ and h. r_i is calculated using the specific resistance of frog Ringer's fluid (90 Ωcm) and the measured capillary radius. The average thickness of the mesentery was earlier determined to be 12.2 μm (Frøkjær-Jensen and Christensen, 1979). This value was based on a shrinkage in microscopical specimens of ~20%. It was later found that the shrinkage was <2% and that the correct value for the average interstitial thickness is therefore 10.0 μm.

The influence of the mesentery and interstitium on the calculation of R_m is given by the figures within the brackets in Eq. 10. The first of the two terms refers to the combined effect of interstitium and its covering mesothelial layer. It would be one if the potential just outside the capillary were zero. The second term refers to the influence of the mesothelial layer covering the upper surface of the capillary. The numerical aspects of the "correction" terms are discussed below on the basis of the actual experimental results.

When the electrode penetrates the endothelial wall, it may leave a rupture through which current can enter the endothelial cell. Since gap junctions between endothelial cells in arterial capillaries have been demonstrated (Simionescu et al., 1975 *a*, and Footnote 1), current may spread within the capillary wall in these vessels, a possibility that has not been considered in the modeling; the lumen diameter is, however, much larger than the thickness of the endothelial cell layer (0.5 μm), so the resistance per centimeter of the cells is much larger than that of the capillary, which, in itself, reduces the problem.

The resistance of the capillary wall is treated as a continuously distributed quantity, because current leaks via the interendothelial junctions, which are organized randomly in a meshwork around the circumference.[1] This situation does not correspond to the regular spacing observed by Frömter and Diamond (1972) in the gallbladder mounted as a flat sheet. The topology of the capillary wall cannot be exactly modeled, and the resistance is considered to be evenly distributed as a first approximation.

METHODS

Preparation

All experiments were carried out on mesenteric capillaries of *Rana temporaria* at room temperature (20–23°C). The animals had been kept for various periods (weeks to months) at 4°C. Experiments were conducted throughout the year. The frog weight was ~40 g. Anesthesia was established by placing the frogs in 5% urethane until mouth respiration stopped. Frogs were then rinsed under water, the abdomen was opened, and the mesentery was prepared for microscopy as described earlier (Crone et al., 1978). Most of the procedure was the same as that given in our earlier paper (Crone et al., 1978), and only special features of the present technique will be described in detail.

The mesentery was observed through a Leitz Laborlux II binocular microscope (Leitz, Wetzlar, W. Germany) using total magnifications between 40 and 320 ×. By means of long-distance objectives (Achromat L 20/0·32, L 32/0·40) working distances of >3 mm were achieved; this made it rather easy to bring microelectrodes mounted on Leitz micromanipulators into contact with the preparation. One of the eyepieces contained a 20 × 20 grid. The side of a square was 120 μm at 40 × magnification and 15 μm at 320 × magnification.

Due to the very fine tip diameter of the microelectrodes penetration through the mesothelium and into the capillary lumen was easy and could be carried out without a holding rod to fix the mesentery. Two microelectrodes were used, one for injection of current and one for potential measurements. The position of the tip of the current electrode and of the potential electrode was read in Cartesian coordinates, and the distance was calculated by Pythagoras's rule. Measurements were performed on various types of capillaries, arterial, mid-capillaries, and venous. Vessels belong to the diverging part of the microvasculature were named "arterial," "mid-capillaries" refers to that portion of the bed where there were no further divisions or confluences, and "venous capillaries" were vessels at which two or more vessels converged.

The superfusate consisted of normal frog Ringer's solution with the following ionic concentrations (mM): Na^+, 110.7; K^+, 2.0; Ca^{2+}, 1.8; and HCO_3^-, 1.2. The osmolality was 215 mosM l^{-1}. Albumin was not added to the superfusate.

The potential readings were always carried out with liberal superfusion (to ensure isopotential conditions on the upper surface of the mesentery). The superfusion had to be interrupted whenever the microelectrodes were repositioned because of focussing problems due to the presence of the stirred superfusate.

The micromanipulators and the microscope were fastened to a common aluminum plate placed on a vibration-free table resting directly on the concrete pillars of the

[1] Bundgaard, M., and J. Frøkjær-Jensen. Functional aspects of the ultrastructure of terminal blood vessels. A quantitative study on consecutive segments of the frog mesenteric microvasculature. Submitted for publication.

building through holes in the floor, thus avoiding stray vibrations due to mechanical disturbances.

The duration of the experiments after exposure of the mesentery was ~2–4 h.

Electrical Measurements

The general design of the experiment is shown in Fig. 2. Current was injected through a glass microelectrode filled with 2 M KCl. The resulting electrical potential displacements were monitored with another microelectrode positioned in various places within the capillary (to measure λ_x) as well as outside the capillary within the two mesothelial membranes (to measure λ_y). The electrical resistance of the electrodes varied between 5 and 10 MΩ, somewhat lower for the current-injection electrode than for that used for potential measurements. The current was delivered through a current-injection unit that passed a constant current of 0.1–0.5 μA for a command voltage of 0.2–1 V.

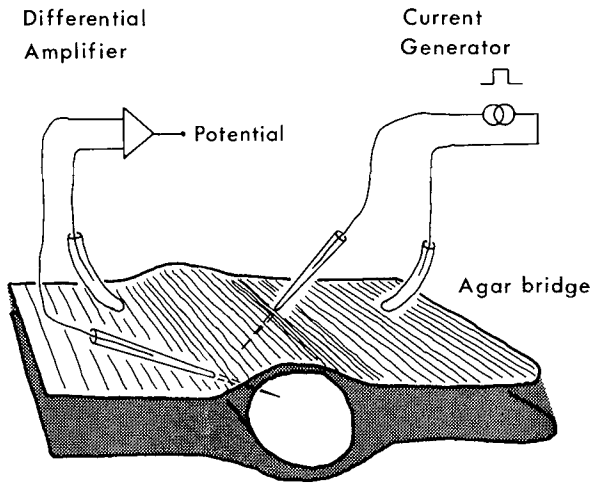

FIGURE 2. Schematic representation of the experimental setup. Square-wave current pulses are injected into a capillary via a glass microelectrode. The electrical potential within the capillary is measured with a second glass microelectrode connected to a high-impedance differential electrometer (and oscilloscope) via a Ag-AgCl wire.

The current-injection unit allowed delivery of this current through electrode resistances up to 20 MΩ. The main resistance for the passage of current was offered by the microelectrode. Problems sometimes arose from an increasing electrical resistance in the tip of the current microelectrode, possibly because of plugging of the tip.

The current circuit was closed via an agar bridge filled with 2 M KCl connected to a Ag-AgCl wire. The agar bridge consisted of a short plastic tube, with an outer diameter of 1.2 mm, containing solidified 2% agar. The whole measuring and current delivery system was kept floating with respect to earth. Thus, the frog was electrically isolated from the conducting parts of the microscope stage by a nonconducting plate fastened to the stage. All other possible connections were effectively isolated from ground. Distortion from electrical mains was minimized by the use of screened leads throughout the laboratory building. The electrical potentials were monitored with a high-impedance differential electrometer. The potential was measured between a

separate agar bridge and the microelectrode tip (cf. Fig. 2). The input impedance of the electrometer was 10^{13} Ω, and the time constant of the system was ~10 ms. Current pulses with a frequency of 2 Hz and a duration of 200 ms were generally used.

The microelectrode potentials were displayed on a storage oscilloscope (OS 4000, Gould Advance, Hainault, Essex, England), from which readings were made. Current strength and overall resistance were constantly monitored on an oscilloscope with storage possibility (Tektronix, Inc., Beaverton, Oreg.). Sometimes the signals were displayed on a two-channel Brush recorder (Gould Inc., Systems Division, Cleveland, Ohio).

Length constants were measured by taking four to five potential readings and plotting the data on semilogarithmic paper. Linearization was performed graphically.

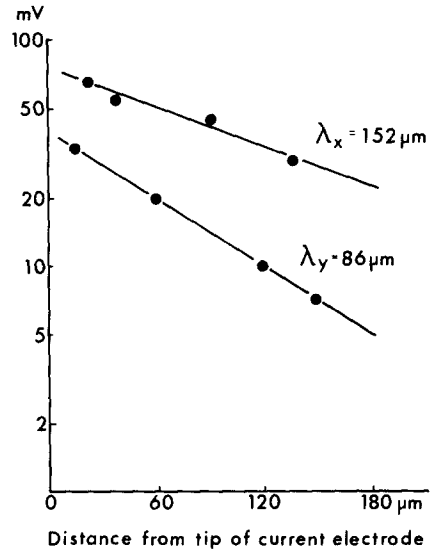

FIGURE 3. Electrical potentials in response to current injections into a mesenteric capillary. (*Upper curve*) Potentials within the capillary at four distances from the current electrode tip. (*Lower curve*) Potentials within the mesentery perpendicular to the capillary wall. The results are from exp. 2, Table IA. The current strength was 2 μA, the duration 200 ms. The vessel's radius was 15 μm. The ordinate shows electrical potentials in millivolts and the abscissa gives distance from the tip of the current electrode in micrometers.

The theoretically predicted electrical potential field in the mesentery is characterized by an exponential decay away from the current electrode. Therefore, in all experiments, we selected vessels that were distant from neighboring vessels, to obtain a potential that was undisturbed by electrical pathways of high conductance.

It was important to verify that the actual potential distribution corresponded to the theoretically predicted behavior. In support of the potential variation proposed in the model we have the following evidence: the potential showed an exponential decline with distance from the current-injecting electrode, both in the capillary and perpendicular to the capillary in the mesentery (Fig. 3); the length constant, λ_x, was the same when measured in the capillary as when measured in the mesentery, parallel

to the capillary. In separate experiments it was confirmed that the potential showed symmetry with respect to the coordinate axes.

The voltage divider ratio was conveniently evaluated by first taking a potential reading in the capillary and subsequently withdrawing the exploring electrode to the outside of the capillary wall. To reduce a possible current leak at earlier puncture sites, measurements began at a remote point from the current electrode and were successively made at closer distances.

The optical diameter of the experimental vessel was measured at the greatest magnification as the distance between two sharp contours. In most cases there was hardly any variation in the optical diameter within the segment chosen for investigation.

The actual conditions differed from those assumed in the model analysis in one respect. The potential at remote distances in the mesentery did not fall to zero but approximated a constant value of ~10% of the initial value close to the capillary. The residual potential was the same when measured in the interstitium as when measured in the superfusate on top of the mesentery. This reflects residual resistance in the superfusate. However, because this nonideality was of borderline significance, it was disregarded in the data evaluation.

RESULTS

Determination of the electrical resistance of the capillary wall in the mesentery requires measurement of the following parameters: (1) The internal resistance of the capillary, r_i, (2) the length constant, λ_x, of the capillary wall, (3) the length constant, λ_y, in the mesentery perpendicular to the capillary, and (4) the voltage divider ratio across the capillary wall. The values for these four parameters, when inserted into Eq. 10 and Eq. 11 allow calculation of the capillary wall resistance.

27 capillaries (arterial and mid-/venous capillaries) were characterized, and the individual results are shown in Tables IA and IB. This number represents less than one-third of the vessels that were submitted to investigation, but many had to be left out because of various problems encountered during the investigations. Sometimes unwanted ground leads that short-circuited the potentials occurred; sometimes a sufficient number of measurements could not be carried out on the same capillary. Thrombi occasionally formed around the current electrode and led to interference with the free flow in the vessel. Free flow was considered important, and measurements on vessels in which stasis with erythrocyte aggregation occurred had to be discontinued.

The results in Tables IA and IB are grouped in two relatively distinct populations consisting of arterial capillaries (Table IA) and mid-/venous capillaries (Table IB), which have different characteristics.

1) The *internal resistance* was derived from the electrical resistance of frog plasma and the capillary cross-sectional area. Because the radius enters with a second power, it influences the resistance quite strongly. There are unavoidable uncertainties in delineating the internal boundaries of capillaries by microscopy in vivo. In an earlier series the radius varied between 8 and 23 μm (Crone et al. 1978), similar to the present range. The tables show the values for optically determined radii in the reported experiments. For an average

TABLE IA

MORPHOLOGICAL AND ELECTRICAL VARIABLES OF ARTERIAL CAPILLARIES

Exp.	Radius	λ_x	λ_y	$V_{out}/V(x)$	R_m
	10^{-4}cm	10^{-4}cm	10^{-4}cm		Ωcm^2
1	15	58	75	0.59	0.68
2	15	152	86	0.46	4.91
6	15	106	95	0.50	2.31
9	15	98	79	0.70	1.12
15	7.5	87	67	0.67	4.51
18	7.5	70	58	0.40	4.08
20	15	101	81	0.72	1.09
25	22	151	91	0.34	3.63
26	11	69	56	0.71	0.93
27	12	159	119	0.39	8.62
Median		99	80	0.54	3.0
Percentiles		70–128	63–89	0.40–0.69	1.0–4.3

Experimental values determined by intracapillary current injection and measurement of intra- and extracapillary electrical potential variations. Intracapillary resistance was calculated from capillary radius and specific resistance of frog plasma (90 Ωcm). λ_x is length constant of capillary in situ. λ_y is length constant of mesenteric interstitium. $V_{out}/V(x)$ is ratio of electrical potential immediately outside capillary to that inside (voltage divider ratio). R_m is the specific resistance of capillary endothelium. Percentiles are 25th and 75th.

TABLE IB

MORPHOLOGICAL AND ELECTRICAL VARIABLES OF MID- AND VENOUS CAPILLARIES

Exp.	Radius	λ_x	λ_y	$V_{out}/V(x)$	R_m
	10^{-4}cm	10^{-4}cm	10^{-4}cm		Ωcm^2
3	15	60	92	0.48	0.97
4	12	50	44	0.36	1.23
5	10	41	44	0.50	0.83
7	15	45	60	0.49	0.58
8	15	65	134	0.76	0.48
10	9	41	78	0.53	0.95
11	8	64	102	0.67	1.64
12	8	57	85	0.67	1.32
13	12	105	119	0.45	3.61
14	12	57	62	0.63	0.80
16	11	43	108	0.70	0.49
17	10	45	60	0.72	0.52
19	18	82	57	0.50	1.18
21	12	64	75	0.63	0.97
22	12.5	39	50	0.52	0.54
23	12.5	60	51	0.50	1.16
24	12	57	54	0.63	0.80
Median		57	62	0.53	0.95
Percentiles		44–63	52–90	0.49–0.66	0.55–1.2

(For table text, see Table IA.)

capillary radius of 12.6 μm the internal resistance, r_i, would be 18.9×10^6 Ωcm^{-1}. The radii of the arterial capillaries tended to be a little larger than those of the other group.

The specific resistance of frog plasma was used instead of that of frog blood because the hematocrit is very low in animals kept in the laboratory. The small vessel hematocrit is lower than that of the large vessels and varies from capillary to capillary, so that meaningful corrections cannot be applied. The error committed by using plasma rather than some fraction of the resistance of blood must be very small.

2) The *length constant*, λ_x, was determined with the current electrode in a fixed position and the potential electrode inserted at various distances from it as decribed above. The distance between the nearest and the most distant measuring point averaged 116 μm, i.e., about two length constants, so that the potential at the most remote position had declined to 10% of the initial value.

The values are given in Tables IA and IB. The average value for the arterial vessels was 99 μm, whereas that of mid- or venous capillaries was 57 μm. The length constants were six to seven times the mean of the capillary radii. Thus, it is possible to make a safe determination of this value (Eisenberg and Johnson, 1970), and the situation is a little more favorable than that encountered in a very leaky epithelium such as mammalian proximal kidney tubule (Boulpaep and Seely, 1971), where the length constants are closer to the internal radius of the tubule.

The effect of the mesothelial covering is to increase the length constant above that for a naked capillary and, although the presence of the mesothelial membranes complicates the formal analysis, it increases the length constant sufficiently to make the conditions experimentally manageable.

3) The *length constant*, λ_y, *in the mesentery* was determined with the stimulating electrode within the capillary and potential determinations at distances from 0 to 180 μm from the capillary wall. The values obtained are shown in Tables IA and IB. The average length constants were 80 and 62 μm, respectively. Their values are determined by a combination of interstitial resistance and mesothelial resistance, as described under Theory. Although the individual data points defined a line in a semilogarithmic plot, data points occasionally fell outside this line. This is probably due to errors in the placement of the electrode tip between the two leaflets of the mesothelial cells lining the interstitium—the electrode tip itself being invisible. Furthermore, the measurements were made under liberal superfusion (to reduce the external electrical resistance), and this could lead to electrode displacement.

4) The *voltage divider ratio across the capillary wall* gives the fraction of the internal potential found just outside the capillary. About 40–50% of the total resistance from stimulating electrode to ground was situated in the capillary membrane. The individual determinations are shown in Tables IA and IB. There was no clear difference in voltage ratio between the two groups.

5) The values in Tables IA and IB show that the *electrical resistance of the capillary wall* was different in the two groups of capillaries, with the arterial

vessels having a somewhat higher electrical resistance. The median values for the two groups were 3.0 Ωcm^2 and 0.95 Ωcm^2, respectively. There was only little overlap between the values in the two groups, and the median values were significantly different, $P < 0.005$ (Wilcoxon's rank test, Snedecor and Cochran [1967]). We have not used statistics based on normal distribution because of the rather small sample sizes, but also because the populations are not necessarily normally distributed. The problem is insufficiently understood at the present time, but long "tails" in distribution curves of capillary permeabilities or filtration coefficients have been noticed by several investigators (Mason et al., 1977; Curry, 1979).

The difference between the two groups of consecutive vessels should not be overemphasized, but it can hardly be doubted that there is a real decrease in electrical resistance along the microvasculature. Curry (1979) noticed a tendency toward lower permeabilities of NaCl in frog mesenteric arterial microvessels compared with more distant locations, and Fraser et al. (1978) found an even more pronounced increase in filtration permeability toward the venous end, with ratios of venous/arterial coefficients of 4–5 (cf. Intaglietta [1967]). Our data indicate that permeability increases by a factor of three from the arteriolar to the venous end.

Accessory data

From the values of λ_x and r_i one can calculate the total input resistance "seen" by the current electrode. The total input resistance, $r_{tot} = 0.5(\lambda_x \cdot r_i)$ (Jack et al., 1975). The mean value of r_{tot} in all determinations was 77 kΩ. As shown in the Appendix, it is possible to derive values for the mesothelial resistance R_{mes} and for the specific interstitial resistance ρ_o. The mean value for R_{mes} was 9.6 Ωcm^2 (all determinations), which is about half of the value found by Frøkjær-Jensen and Christensen (1979). However, R_{mes} is inversely proportional to the capillary radius, and some of the discrepancy may arise from slight overestimation of vessel radius. Also, the continued superfusion with albumin-free frog Ringer's solution may have led to increased permeability (Mason et al., 1977).

The mean value of ρ_o was 273 Ωcm (all determinations). The ratio between the resistivity of frog Ringer's solution and the resistivity of the interstitium was 0.33. We have earlier determined an interstitial K^+ diffusion coefficient of 0.63×10^{-5} $cm^2 s^{-1}$ (Crone et al., 1978). The free diffusion coefficient at 20°C for potassium is 1.8×10^{-5} $cm^2 s^{-1}$, so that the interstitial diffusion coefficient is 0.35 of the free diffusion coefficient. Both the present and previous determinations suggest a reduction of interstitial diffusion (or conductivity) by a factor of 3 due to tortuosity effects.

The length constant of the mesothelial cell layer, λ_{mes}, was determined in each case from the data in the tables. The mean value of all determinations was 51.5 μm. As mentioned in the Appendix, λ_{mes} should equal the length constant λ, determined in our earlier paper on potassium permeability of mesenteric capillaries (Crone et al., 1978). The condition for this to be true is that restriction in mesothelial permeation is the same for the sodium and

chloride ions that largely carry the current in the present experiment as for potassium ions. The mean value for λ obtained earlier was 60.2 μm (Crone et al., 1978), in satisfactory agreement with the present findings.

DISCUSSION

For clarity, we discuss, in turn, the analysis, the data, and the implications of these experiments.

Analysis

As described above, the determination of the electrical resistance of a capillary wall was based on elementary cable considerations supplemented with terms necessitated by the special geometric conditions. A discussion of the particular model we have used may begin with the equation for a naked capillary: $r_m = r_i \cdot \lambda^2$. For the mesenteric capillary this relation is replaced by Eq. 10, which has the same structure except that there is a multiplication factor added to account for the geometric conditions. Eq. 10 states that $r_{lat} = r_i \cdot \lambda_x^2 \cdot (\alpha + \beta)$. The first correction factor, α, gives the voltage drop across the capillary wall as fraction of the voltage inside the capillary. This accounts for the effect of the distributed resistance outside the capillary wall. The factor would be unity if the interstitial potential were zero; however, this is not the case, and the factor is smaller than unity (cf. Tables IA and IB). The product $h \cdot \lambda_y$, which determines the deviation from unity, depends on the ratio, h, between the resistivity of the interstitium and that of the capillary wall and also upon λ_y, which is mainly determined by the resistance of the mesothelial membrane. The mean value of α was 0.43. The second correction term, β, refers to the fraction of current leaking in the upward direction through the combined capillary and mesothelial resistance. The mean value of β was about half that of α, 0.22. The combined effect of the two correction terms in the brackets was to reduce the capillary wall resistance by ~30% from a situation in which these factors had been disregarded and the capillary treated as a naked capillary. In other words, according to the two-dimensional model employed in the present case, current only leaks out via a certain fraction of the entire circumference, in contrast to the naked capillary.

A numerical example may illustrate this. Assuming that the capillary has a radius of 10^{-3} cm and that the mesenteric thickness is also 10^{-3} cm, $\lambda_x = 60 \times 10^{-4}$ cm, $\lambda_y = 90 \times 10^{-4}$ cm, and the ratio of potential outside/inside is 0.5. This set of parameter values gives: $r_i = 29.0$ MΩcm^{-1}, $h = 111$ cm^{-1}, $h\lambda_y = 1.0$, $r_{lat} = 774$ Ωcm, and $R_m = 1.55$ Ωcm^2. For a naked capillary, the length constant would be only 29×10^{-4} cm instead of 60×10^{-4} cm, as calculated when the effect of the mesothelium is taken into consideration. The mesothelium acts as a barrier that limits the current leakage from the capillary and hence increases the length constant. Because the mesenteric capillary is a very leaky type of capillary, one must expect that many other types of capillaries, being less permeable, could be submitted to cable analysis if it were technically feasible to insert microelectrodes into them. However, a serious complication

may arise from the very large internal resistance in capillaries with significantly smaller diameters, such as mammalian capillaries.

The value that most decisively influences the numerical value of the capillary resistance is the capillary radius because it enters with a second power since $r_i = \rho_i/\pi a^2$. The mean radius in the present series was 12.6 μm. Mason et al. (1979) give 10 μm as the average value in the frog mesentery. Bundgaard and Frøkjær-Jensen[1] studied the consecutive segments and found small systematic variations in radius with a mean value of 9.9 μm in arteriolar capillaries, similar to that in venous (pericytic) capillaries, whereas mid-capillaries had a radius of 7.5 μm. There is no doubt that there is some bias in the selection of vessels for single capillary studies in favor of larger vessels at the expense of the smallest capillaries because they are more difficult to work with. This applies to our study and, judging from their mean figures, also to those of Michel et al. (1974) and the original experiments of Landis (1927). Thus, we have no strong reason to introduce correction factors for the optically determined radii given in Tables IA and IB.

In view of the relatively complicated model of the combined capillary-mesentery system, it is of interest to quantify the effect upon the results of further simplifying the model. If the effect of current leak through the upper part of the capillary, as well as the interstitial resistance, is neglected current would leak in the lateral direction through a capillary membrane with an average height, d, corresponding to that of the interstitium (=10 μm) into zero potential. In this case, only r_i and λ_x had to be determined, since $r_i \cdot \lambda_x^2 = r_{lat}$ and $R_m = 2dr_{lat}$. The model is thus reduced to one dimension, which gives an easier experimental situation. The median value for R_m in mid-/venous capillaries using this analysis would be 1.2 Ωcm^2 (against 0.95 Ωcm^2), which means that a very simplified model would still give acceptable values.

The mesenteric capillary—despite its popularity—belongs to an experimentally difficult group of microvessels because of the complications resulting from the mesothelial covering. In current studies of the capillaries at the surface of the frog brain, one-dimensional cable analysis was sufficient, and the experimental conditions were greatly improved because of the tightness of brain capillary endothelium, which has an electrical resistance of ~1,300 Ωcm^2 (Crone and Olesen, 1981).

Data

Several aspects of the data were discussed in the presentation of the experimental results, but some supplementary comments may be added.

One of the advantages of experiments on single capillaries is that the technique allows *regional* investigation of permeability, whereas whole-organ experiments give information about all permeable segments lumped together. We found that the electrical resistance of arterial capillaries was higher by a factor of 3 than that of those vessels placed more distally in the capillary bed. This ratio corresponds well with measurements of hydraulic conductivity in consecutive microvascular segments. Thus, Fraser et al. (1978) found an inverse relationship between intravascular pressure and hydraulic conductiv-

ity. This functional characteristic apparently applies also to diffusional permeability of small solutes. That the permeability ratio is about 3 for both hydraulic and diffusional permeability suggests that the phenomenon is due to a variation in fractional open slit length rather than to variations in slit width. Had larger slits been present in the venous end, one would have expected a steeper increase in hydraulic conductivity if Poiseuillean flow takes place during transcapillary filtration.

Though the data from mid- and venous capillaries cluster around a relatively narrow range of resistances, this is not so for the arterial resistances, where the range is much larger. The explanation for this difference in heterogeneity is not clear.

The different wall resistances of the two populations is reflected in the capillary length constant, λ_x. The ratio between wall resistances in the two groups should approximately correspond to the squared ratio of the length constants. The resistance ratio was $3.0/0.95 = 3.2$; the squared ratio between the length constants was $(99/57)^2 = 3.0$, in good agreement with theory.

The solution for the model used in the data analysis assumes that resistance of the membrane is independent of position. Because the resistance falls three times from arterial to venous vessels, this assumption is not wholly fulfilled. However, with a length constant of <100 μm and distances from arterial to venous vessels from 500 to 1,000 μm, the change in resistance within a given segment is negligible.

The transverse length constants, λ_y, of the two sets of measurements are not significantly different. Although the median values are seemingly different, the ranges given by the percentiles are similar (Tables IA and IB).

At first it is surprising that the voltage divider ratio, $V_{out}/V(x)$, does not differ between the two groups. The voltage ratio is the ratio $R_{out}/(R_m + R_{out})$, where R_{out} is the external resistance as seen from the outside of the capillary wall ($=\lambda_y \cdot \rho_o$). This ratio decreases with increasing wall resistance, so that one would expect a smaller ratio in arterial vessels, everything else being equal. Apparently, the variations of the resistance in the interstitium and in the mesothelial membrane override the influence of R_m, with the consequence that the difference is only seen in the lower percentile (cf. Tables IA and IB).

Implications

Three aspects of our results on capillary wall electrical resistance will be discussed: (1) relation to earlier determinations of ionic permeability, (2) relation to electrical resistance of some leaky epithelia, and (3) correlation of morphology and electrical resistance leading to an equivalent model of the capillary wall that accounts for the observed electrical resistance and earlier determinations of filtration coefficients.

1) Two series of measurements of *ionic permeability* of frog mesenteric capillaries have been reported, with $P_K = 67 \times 10^{-5}$ cm·s^{-1} (Crone et al., 1978) and $P_{NaCl} = 44 \times 10^{-5}$ cm·s^{-1} (Curry, 1979). In neither of these studies were arterial and mid-/venous capillaries treated separately, although Curry noticed the trend toward lower values in arterial vessels. To compare our earlier

determinations of ionic permeability with present results, we used the average resistance from all vessels, 1.85 Ωcm^2, because we did not distinguish between permeabilities in consecutive segments in the earlier study.

a) Under conditions of flux equilibrium the partial conductance, $G_j = c_j \cdot P_j \cdot (F^2/RT)$ (Sten-Knudsen, 1978). The transcapillary conductance of a KCl solution isomostic with frog Ringers solution would be $0.2 \times 10^{-3} \times 67 \times 10^{-5} \times 3{,}754 \times 10^3$ $mol \cdot cm^{-3} \cdot cm \cdot s^{-1} \cdot coulomb \cdot V^{-1} \cdot mol^{-1} = 0.54$ $\Omega^{-1} \cdot cm^{-2}$, equivalent to a resistance of 1.84 Ωcm^2 (using $P_K = 67 \cdot 10^{-5}$ $cm \cdot s^{-1}$). Because the main cation in frog plasma is Na^+, which has a smaller mobility than K^+, it is to be expected that the actual resistance would be a little higher. In view of the large range of the experimental determinations of resistance, there is, however, satisfactory correspondence between the actual measurements and the implications of earlier studies of ionic permeability in single capillaries.

b) If it is assumed that the medium that carries the current through the capillary wall has a specific resistance similar to that of frog plasma (90 Ωcm), an equivalent electrical resistance can be calculated using the above P_K value. Because $P_K/D_K = 67 \times 10^{-5}/1.80 \times 10^{-5} = 38.9$ $cm^{-1} = A_p/\Delta x$, where A_p is pore area per square centimeter of capillary surface and Δx is the pore diffusion distance, the expected electrical resistance is given by $90/38.9 = 2.3$ Ωcm^2, which also compares quite well with the overall electrical resistance. That the calculated resistance comes out a little higher than that for the pure KCl case may be explained by the smaller mobility of Na.

That the electrical resistance of mid-/venous capillaries was somewhat lower (0.95 Ωcm^2) indicates that the ionic permeabilities in this vascular segment are even higher than our previously reported average figure of P_K, although this figure was about 10 times higher than that known from whole-organ studies of mammalian muscle capillaries. In a discussion of capillary pore models, and on the basis of theoretical considerations, Curry (1980) reached the conclusion that our value of P_K may eventually be on the low side. Our present results from mid-venous capillaries support his expectation.

2) The idea that there are *similarities between endothelia and epithelia*, as far as passive permeability properties are concerned, has been advanced several times (Crone, 1977 and 1981). It is now possible to scrutinize this proposal in greater detail, because electrical properties and ionic permeabilities of several epithelia are well known. Table II summarizes some values. It can be seen that the present endothelium has the lowest resistance and highest ionic permeability. At first glance however, it is surprising that even a *very* permeable capillary, such as the present one, has a resistance only about five times lower than that of a renal tubular epithelium. That the mammalian kidney epithelium is completely impermeable to inulin (and sucrose), whereas such non-electrolytes pass easily through capillary endothelia, raises some intriguing questions about the mechanics of pore permeation or of the microstructure of epithelial and endothelial pores (Michel, 1980).

A little more can be said about the decreasing electrical resistance in consecutive segments of microvessels. Simionescu et al. (1975 *a*), using freeze-

fracture technique in studies of consecutive segments in rat mesentery, showed that the arterial microvessels have tighter junctions with a greater number of ridges than do true capillaries or pericytic venules. The junctions in venular capillaries were found to be particularly loose, with only one intramembranous "strand" and few particulate structures. Unfortunately, the lack of a true understanding of the relation of ultrastructural features to permeability precludes quantitative considerations (Martínez-Palomo and Erlij, 1975; Hull and Staehelin, 1976).

3) In our earlier work (Crone et al., 1978), we put forward the possibility that the *porous pathways for transcapillary transport of ions and small solutes* were identical to the "transendothelial channels" described by Simionescu et al. (1975 *b*). Despite intense efforts to localize such channels in frog mesenteric

TABLE II

ELECTRICAL RESISTANCES AND ION PERMEABILITIES OF ENDOTHELIA AND EPITHELIA

Tissue	Electrical resistance	Reference	K^+ or Na^+ permeability	Reference
	Ωcm^2		$cm\ s^{-1}$	
Brain endothelium	1300	Crone and Olesen, 1891	3×10^{-7}	Hansen et al., 1977
Necturus proximal tubule	70	Boulpaep, 1972	3×10^{-6}	Boulpaep, 1972
Rat proximal tubule	5	Hegel et al., 1967	2.3×10^{-5}	Schafer et al., 1974
Frog mesenteric endothelium	1–3	Present article	6.7×10^{-4}	Crone et al., 1978

Comparison of electrical resistances and ion permeabilities of endothelia and "leaky" epithelia. Apparently, there is a large variation in permeabilities (and probably in electrical resistance) among various endothelia, because the brain capillaries have ion permeabilities just as low as "tight" epithelia.

capillaries, we have not been able to provide the necessary experimental support (Bundgaard et al., 1979 *a* and 1979 *b*; Frøkjær-Jensen, 1981). Therefore, we have been forced to resume the idea of the interendothelial cleft as the principal pathway for small-solute transport. The main reason for choosing the interendothelial cleft is that it is unlikely that the plasma membrane of the endothelial cells would allow significant current pasage. Furthermore, studies with electron-dense tracers show that passage through the cleft is possible, albeit with pronounced delay for large test molecules (Karnovsky, 1970; Wissig, 1979) such as peroxidase (equivalent diameter, 50 Å). The stumbling block for immediately accepting the interendothelial cleft as *the* hydrophilic pathway is the presence of what appears in many instances to be a closed "tight junction" (zonula occludens). Palade et al. (1979), reviewing the morphology of transcapillary passage, indicate that solutes with molecular diameters below 10 Å probably can pass the tight regions. The tight junctions in frog mesenteric capillaries do not seal neighboring endothelial cells together throughout the entire circumference, since many sections show a continuous

open passageway (Mason et al., 1979; and footnote 1). The width of the paracellular pathway is larger in the venous capillaries (Simionescu et al., 1978).

It is tempting to characterize an equivalent interendothelial slit that would explain the observed electrical resistances. The more so, since morphometric studies in our laboratory have provided a number for the total slit length per square centimeter of capillary surface area, averaging ~1,600–2,400 cm/cm^2.[1]

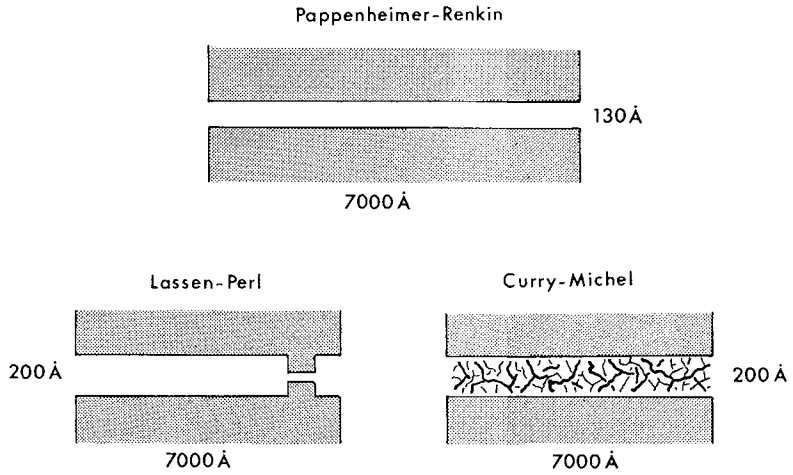

FIGURE 4. Three alternative pore models. The Pappenheimer-Renkin model proposes slits with parallel plates (Pappenheimer, 1953). The dimensions would explain present findings and give a filtration coefficient as previously determined by Curry et al. (1976). The Lassen-Perl model (Lassen and Trap-Jensen, 1970; Perl, 1971) assumes obligatory passage through two consecutive segments, one of which is narrowed down to a width of 50 Å while the other has a width of 200 Å. It is not known whether the regions of "tight" junctions constitute circumferential belts around the endothelial cells or whether they are discontinuous, in which case modeling would be rather arbitrary. The Curry-Michel model (Curry, 1980; Michel, 1980) places an important diffusion and filtration hindrance within the pore in the form of a matrix with characteristics that can explain selective diffusion restriction and measured solute reflection coefficients. It postulates creeping flow in the pore rather than Poiseuillean flow. The cleft depth of 0.7 μm refers to measurements on frog mesenteric capillaries.[1]

This new value for the mesenteric capillary places an upper limit on the area available for transcapillary passage of current (under the proviso that the dominant current leak is via the paracellular junctions). With a total slit length of 2,000 cm/cm^2, an equivalent slit width of 13 nm, and a cleft depth of 0.7 μm, an electrical resistance of (90 × 7,000/130 × 2,000) = 2.4 Ωcm^2 is calculated for a capillary wall with frog Ringer's solution in the junctions, a figure which is close to our overall average of 1.85 Ωcm^2.

Because some of the foundations of the classical pore theory (Pappenheimer,

1953) are under current discussion and alternative theories of pore permeation are being advanced (Curry, 1980; Michel, 1980), it is, perhaps, not profitable to go further in slit modeling. Fig. 4 summarizes three versions of the interendothelial equivalent "pore" geometry. With suitable dimensions, any of the three proposals could comply with the observed electrical resistances (and earlier determinations of filtration coefficients of frog mesenteric capillaries).

We will leave the pore alternatives as interesting speculations among which we cannot choose on the basis of present evidence. The main interest in our new values does not particularly lie in their significance for pore modeling but rather in the prospects the technique gives for future research on single capillaries in other tissues. We have shown that the electrical resistance complies well with earlier determination of potassium permeability, indicating that the high-potassium solutions did not artificially increase permeability. We have characterized a segmental variation in solute permeability and described a method that may allow rapid changes in capillary permeability to be studied. It extends the catalogue of approaches to permeability of single capillaries and should be useful in cases in which ion-sensitive microelectrode technique cannot be applied or is unnecessary.

APPENDIX

The relationship between R_m, R_{mes}, and ρ_o and the experimentally determined parameters λ_x, λ_y, and h is derived as follows. The factor $h\lambda_y/(1 + h\lambda_y)$ of Eq. 9*b* has been determined using the boundary condition (Eq. 8).

When solution (Eq. 9*b*) is inserted into the field equation for the interstitium, Eq. 7, one obtains

$$\frac{1}{\lambda_x^2} + \frac{1}{\lambda_y^2} = \frac{1}{\lambda_{mes}^2}, \tag{A1}$$

with $\lambda_{mes} = \sqrt{R_{mes}/r_o}$.

Apart from possible differences in permeation restriction for Na, K, and Cl in the mesothelial membrane, R_{mes} is inversely proportional to the mesothelial permeability, P_m, and ρ_o is inversely proportional to the interstitial diffusion constant D_i. Thus, $\lambda_{mes} = \sqrt{D_i \cdot d/P_m}$. λ_{mes} is identical to the diffusion length introduced in the "interstitial diffusion method" (Crone et al., 1978).

A second relation is obtained by inserting the solutions (Eqs. 9*a* and 9*b*) into the field equation for the capillary, Eq. 4.

$$\frac{1}{r_i\lambda_x^2} = \frac{1}{r_{lat}} \cdot \frac{1}{1 + h\lambda_y} + \frac{1}{r_{up}}. \tag{A2}$$

In this equation, r_{up} must be expressed by r_{lat} and other measurable quantities. Eq. 6, which defines r_{up}, can thus be expressed as

$$r_{up} = 2 \cdot r_{lat}(d + h\lambda_{mes}^2)/(\pi a - d),$$

where we have used the definitions of the quantities h, r_o, r_{lat}, and λ_{mes}. Substituting r_{up} into Eq. A2 yields the main relation

$$r_{lat} = r_i \cdot \lambda_x^2 \left[\frac{1}{1 + h\lambda_y} + \frac{\pi a - d}{2(d + h\lambda_{mes}^2)} \right]. \tag{10}$$

Once r_{lat} has been determined, the remaining resistances are obtained thus: specific resistance of endothelial wall, $R_m = 2d \cdot r_{lat}$, resistivity of interstitium, $\rho_o = h \cdot R_m$, specific resistance of mesothelial layer, $R_{mes} = \frac{\rho_o}{d} \cdot \lambda_{mes}^2$.

Received for publication 10 July 1980.

REFERENCES

BOULPAEP, E. L., and J. F. SEELY. 1971. Electrophysiology of proximal and distal tubules in the autoperfused dog kidney. *Am. J. Physiol.* **221:**1084–1096.

BOULPAEP, E. L. 1972. Permeability changes of the proximal tubule of *Necturus* during saline loading. *Am. J. Physiol.* **222:**517–531.

BUNDGAARD, M., C. CRONE, and J. FRØKJÆR-JENSEN. 1979 *a*. Extreme rarity of transendothelial channels in the frog mesenteric capillary. *J. Physiol. (Lond.)*. **291:**38P.

BUNDGAARD, M., J. FRØKJÆR-JENSEN, and C. CRONE. 1979 *b*. Endothelial plasmalemmal vesicles as elements in a system of branching invaginations from the cell surface. *Proc. Natl. Acad. Sci. U. S. A.* **76:**6439–6442.

CRONE, C. 1977. Endothelia and epithelia. *In* Microcirculation. J. Grayson and W. Zingg, editors. Plenum Press, New York. **2:**7–10.

CRONE, C. 1980. The electrical resistance of a capillary wall. A new approach to capillary permeability. *J. Physiol. (Lond.)*. **301:**70P–71P.

CRONE, C. 1981. Tight and leaky endothelia. *In* Water Transport across Epithelia. H. H. Ussing, N. Bindslev, N. A. Lassen, and O. Sten-Knudsen, editors. Munksgaard, Copenhagen. In press.

CRONE, C., and J. J. FRIEDMAN. 1976. A method for determining potassium permeability of a single capillary. *Acta Physiol. Scand.* **96:**13A–14A.

CRONE, C. J. FRØKJÆR-JENSEN, J. J. FRIEDMAN, and O. CHRISTENSEN. 1978. The permeability of single capillaries to potassium ions. *J. Gen. Physiol.* **71:**195–220.

CRONE, C., and S. P. OLESEN. 1981. The electrical resistance of brain capillary endothelium. *J. Physiol. (Lond.)*. (Abstr.) In press.

CURRY, F. E. 1979. Permeability coefficients of the capillary wall to low molecular weight hydrophilic solutes measured in single perfused capillaries of frog mesentery. *Microvasc. Res.* **17:**290–308.

CURRY, F. E. 1980. Is the transport of hydrophilic substances across the capillary wall determined by a network of fibrous molecules? *Physiologist.* **23:**90–93.

CURRY, F. E., J. C. MASON, and C. C. MICHEL. 1976. Osmotic reflexion coefficients of capillary walls to low molecular weight hydrophilic solutes measured in single perfused capillaries of the frog mesentery. *J. Physiol. (Lond.)*. **216:**319–336.

EISENBERG, R. S., and E. A. JOHNSON. 1970. Three-dimensional electrical field problems in physiology. *Progr. Biophys. Mol. Biol.* **20:**1–65.

FRASER, P. A., L. H. SMAJE, and A. VERRINDER. 1978. Microvascular pressures and filtration coefficients in the cat mesentery. *J. Physiol. (Lond.)*. **283:**439–456.

FRØKJÆR-JENSEN, J. 1980. Three-dimensional organization of the plasmalemmal vesicles in endothelial cells. An analysis by serial sectioning of frog mesenteric capillaries. *J. Ultrastruct. Res.* **73:**9–20.

FRØKJÆR-JENSEN, J., and O. CHRISTENSEN. 1979. Potassium permeability of the mesothelium of the frog mesentery. *Acta Physiol. Scand.* **105:**228–238.

FRÖMTER, E., and J. M. DIAMOND. 1972. Route of passive ion permeation in epithelia. *Nat. New Biol.* **235**:9–13.

HANSEN, A. J., H. LUND-ANDERSEN, and C. CRONE. 1977. K^+-permeability of the blood-brain barrier. *Acta Physiol. Scand.* **101**:438–445.

HEGEL, U., E. FRÖMTER, and T. WICK. 1967. Der elektrische Wandwiderstand des proximalen Konvolutes der Rattenniere. *Pfluegers Arch. Eur. J. Phyiol.* **294**:274–290.

HODGKIN, A. L., and W. A. H. RUSHTON. 1946. The electrical constants of a crustacean nerve fibre. *Proc. R. Soc. Lond. B Biol. Sci.* **133**:444–479.

HULL, B. E., and L. A. STAEHELIN. 1976. Functional significance of the variations in the geometrical organization of tight junction networks. *J. Cell Biol.* **68**:688–704.

INTAGLIETTA, M. 1967. Evidence for a gradient of permeability in frog mesenteric capillaries. *Bibl. Anat.* **9**:465–468.

JACK, J. J. B., D. NOBLE, and R. W. TSIEN. 1975. Electric Current Flow in Excitable Cells. Clarendon Press. Oxford. 502 pp.

KARNOVSKY, M. J. 1970. Morphology of capillaries with special reference to muscle capillaries. *In* Capillary Permeability. C. Crone and N. A. Lassen, editors. Academic Press, Inc., New York. 341–350.

LANDIS, E. M. 1927. Micro-injection studies of capillary permeability. II. The relation between capillary pressure and the rate at which fluid passes through the walls of single capillaries. *Am. J. Physiol.* **82**:217–238.

LASSEN, N. A., and J. TRAP-JENSEN. 1970. Estimation of the fraction of the inter-endothelial slit which must be open in order to account for the observed transcapillary exchange of small hydrophilic molecules in skeletal muscle in man. *In* Capillary Permeability. C. Crone and N. A. Lassen, editors. Academic Press, New York. 647–653.

MARTÍNEZ-PALOMO, A., and D. ERLIJ. 1975. Structure of tight junctions in epithelia with different permeability. *Proc. Natl. Acad. Sci. U. S. A.* **72**:4487–4491.

MASON, J. C., F. E. CURRY, and C. C. MICHEL. 1977. The effects of proteins upon the filtration coefficient of individually perfused frog mesenteric capillaries. *Microvasc. Res.* **13**:185–202.

MASON, J. C., F. E. CURRY, I. F. WHITE, and C. C. MICHEL. 1979. The ultrastructure of frog mesenteric capillaries of known filtration coefficients. *Q. J. Exp. Physiol. Cogn. Med. Sci.* **64**: 217–224.

MICHEL, C. C. 1980. Filtration coefficients and osmotic reflection coefficients of the walls of single frog mesenteric capillaries. *J. Physiol. (Lond.)*. **309**:341–355.

MICHEL, C. C., J. C. MASON, F. E. CURRY, and J. E. TOOKE. 1974. A development of the Landis technique for measuring the filtration coefficient of individual capillaries in the frog mesentery. *Q. J. Exp. Physiol. Cogn. Med. Sci.* **59**:283–309.

PALADE, G. E., M. SIMIONESCU, and N. SIMIONESCU. 1979. Structural aspects of the permeability of the microvascular endothelium. *Acta Physiol. Scand.* **463**(Suppl.):11–32.

PAPPENHEIMER, J., 1953. Passage of moleculls through capillary walls. *Physiol. Rev.* **33**:387–423.

PERL, W. F. 1971. Modified filtration-permeability model of transcapillary transport—a solution of the Pappenheimer pore puzzle? *Microvasc. Res.* **3**:233–251.

SCHAFER, J. A., S. L. TROUTMAN, and T. E. ANDREOLI. 1974. Volume reabsorption, transepithelial potential differences, and ionic permeability properties in mammalian superficial proximal straight tubules. *J. Gen. Physiol.* **64**:582–607.

SIMIONESCU, M., N. SIMIONESCU, and G. E. PALADE. 1975 *a*. Segmental differentiations of cell junctions in the vascular endothelium. *J. Cell Biol.* **67**:863–885.

SIMIONESCU, N., M. SIMIONESCU, and G. E. PALADE. 1975 *b*. Permeability of muscle capillaries

to small heme-peptides. Evidence for the existence of patent transendothelial channels. *J. Cell Biol.* **64**:586–607.

SIMIONESCU, N., M. SIMIONESCU, and G. E. PALADE. 1978. Open junctions in the endothelium of the postcapillary venules of the diaphragm. *J. Cell Biol.* **79**:27–44.

SNEDECOR, G. W., and W. G. COCHRAN. 1967. Statistical Methods. 6th Edition. The Iowa State University Press, Ames. 1–593.

STEN-KNUDSEN, O. 1978. Passive transport processes. *In* Membrane Transport in Biology. G. Giebisch, D. C. Tosteson, and H. H. Ussing. Springer-Verlag, Berlin. 5–113.

WISSIG, S. L. 1979. Identification of the small pore in muscle capillaries. *Acta Physiol. Scand.* **463**(Suppl.):33–44.